Human induced pluripotent stem cell-derived glial cells and neural progenitors display divergent responses to Zika and dengue infections

Julien Muffat[a,1,2], Yun Li[a,1,3], Attya Omer[a,1], Ann Durbin[b,c,d], Irene Bosch[b,c,d], Grisilda Bakiasi[e], Edward Richards[f], Aaron Meyer[f,4], Lee Gehrke[b,c,d], and Rudolf Jaenisch[a,g,5]

[a]Whitehead Institute for Biomedical Research, Cambridge, MA 02142; [b]Institute for Medical Engineering and Science, Massachusetts Institute of Technology, Cambridge, MA 02139; [c]Department of Microbiology and Immunobiology, Harvard Medical School, Boston, MA 02115; [d]Harvard–MIT Program in Health Sciences and Technology, Cambridge, MA 02139; [e]Department of Biology, Bryn Mawr College, Bryn Mawr, PA 19010; [f]Koch Institute for Integrative Cancer Research at MIT, Cambridge, MA 02139; and [g]Department of Biology, Massachusetts Institute of Technology, Cambridge, MA 02139

Maternal Zika virus (ZIKV) infection during pregnancy is recognized as the cause of an epidemic of microcephaly and other neurological anomalies in human fetuses. It remains unclear how ZIKV accesses the highly vulnerable population of neural progenitors of the fetal central nervous system (CNS), and which cell types of the CNS may be viral reservoirs. In contrast, the related dengue virus (DENV) does not elicit teratogenicity. To model viral interaction with cells of the fetal CNS in vitro, we investigated the tropism of ZIKV and DENV for different induced pluripotent stem cell-derived human cells, with a particular focus on microglia-like cells. We show that ZIKV infected isogenic neural progenitors, astrocytes, and microglia-like cells (pMGLs), but was only cytotoxic to neural progenitors. Infected glial cells propagated ZIKV and maintained ZIKV load over time, leading to viral spread to susceptible cells. DENV triggered stronger immune responses and could be cleared by neural and glial cells more efficiently. pMGLs, when cocultured with neural spheroids, invaded the tissue and, when infected with ZIKV, initiated neural infection. Since microglia derive from primitive macrophages originating in proximity to the maternal vasculature, they may act as a viral reservoir for ZIKV and establish infection of the fetal brain. Infection of immature neural stem cells by invading microglia may occur in the early stages of pregnancy, before angiogenesis in the brain rudiments. Our data are also consistent with ZIKV and DENV affecting the integrity of the blood–brain barrier, thus allowing infection of the brain later in life.

Zika | microglia | organoids | interferon | iPS

Zika virus (ZIKV) emerged in 1947, and had not been considered a grave threat to humans until very recently (1). In 2013, an epidemic in French Polynesia was associated with significant morbidity in the form of Guillain-Barre syndrome (2). Since 2014, the virus has been spreading throughout the Americas and the Caribbean, threatening the southern United States where populations of its mosquito vectors, *Aedes aegyptii* and *Aedes albopictus*, are endemic. Concurrent to the spread of ZIKV in South America, a rise in cases of severe fetal malformations, including microcephaly (3, 4), was rapidly linked to maternal infection, with apparent peak vulnerability during the first trimester of pregnancy (3, 5). While neural progenitor cells (NPCs) have been shown to be highly sensitive to infection (6–9), the current epidemic raises many questions. Why is ZIKV presenting so severely and only now? Sequence variations (10) between the original 1947 Ugandan strain (ZIKV^u) and the current circulating variants are relatively minor, although recent analysis indicates the presence of a novel mutation in the prM protein associated with the currently circulating American strains (11). How does ZIKV accomplish its vertical transmission from mother to fetus despite all defenses in place? The damage to the fetus can be quite variable, possibly pointing to narrow windows of opportunity for the virus to wreak havoc on development.

What makes human hosts so vulnerable, when mice do not develop the disease unless their antiviral defenses are knocked down (12–14)? This latter consideration questions our ability to model the pathology in rodents, as the needs to dampen interferon (IFN) responses make the study of viral spread within the mouse host arduous. What of the vulnerability of more mature nervous systems: Can the virus be completely cleared postnatally, or does it leave neurological sequalae even in absence of overt teratogenicity? Are there circumstances in which ZIKV can reach an adult nervous system from the periphery (2, 15)? The consequence of such an event are largely unknown.

Significance

We describe the ability of the Zika virus to infect various cells of the fetal brain, modeled from induced pluripotent stem cells derived from a patient and grown in identical conditions. Zika is associated with microcephaly, while the similar dengue virus is not. We described differences in the behavior of these two viruses. Zika often fails to trigger efficient antiviral responses, surviving encounters with brain immune cells, and killing immature nerve cell precursors that have poor innate antiviral defenses. Precursors of the brain's immune cells, microglia, circulating in the fetus, may take the virus to the fetal brain where it will stall growth or cause cell death. We show that interferon-γ efficiently protects against this viral transfer.

NEUROSCIENCE

In this report, we address some of these questions using in vitro modeling to study the interaction of ZIKV with various cells of the CNS. We focused our study on the prototypical ZIKV[u] strain, which is well characterized and particularly cytotoxic in vitro (7). We contrast the tropism and cytotoxicity of ZIKV with that of dengue (DENV), a closely related flavivirus (16), for which there are no known reports of teratogenic events. DENV may in some circumstances prove neurotropic and neurovirulent, but the incidence of such pathology is limited. DENV is carried by the same mosquito vectors and is therefore present in overlapping geographic areas. Until the current reemergence of ZIKV, DENV was the most concerning arbovirus in the developing world. De facto, we have much to glean from understanding the differences and similarities between these viruses to therapeutic discovery. The interactions between DENV and ZIKV may be particularly relevant, as many patients contracting ZIKV have already been exposed to DENV.

Results

We generated multiple cell types from human induced pluripotent stem (iPS) cells, allowing derivation from a given donor (17, 18), avoiding confounding effects of genetic background on viral infectivity or cytotoxicity. Microglia, neural progenitors, astrocytes, and neurons, the four CNS cell types used in our study, were derived from the same iPS cells and grown in a common serum-free medium. The cells were infected with the MR766 strain of ZIKV[u], which has been reported to be cytotoxic to human neural progenitors (7, 8). We confirmed that a ZIKV[u] inoculum corresponding to a multiplicity of infection (MOI) of 1 (as measured independently on Vero cells) was highly infective and cytotoxic to iPS-derived neural progenitors (Fig. 1A, Left and SI Appendix, Fig. S1). The cells accumulated large envelope-positive cytoplasmic inclusions and died by caspase-mediated apoptosis (SI Appendix, Fig. S1). When challenged with increasing multiplicities of ZIKV[u], NPCs accumulated viral genome (vRNA) up to twice the levels of endogenous GAPDH (Fig. 1B, Left). When infecting astrocytes, differentiated from NPCs, cells became positive for the ZIKV envelope protein (Fig. 1A, Middle) and produced vRNA in excess of endogenous GAPDH (Fig. 1B, Middle), but virus-induced cell death was not observed (SI Appendix, Fig. S1). iPS-derived microglia-like cells (pMGLs) infected with ZIKV[u] became positive for the ZIKV envelope protein (Fig. 1A, Right) and accumulated vRNA in a dose-dependent manner reaching levels of almost 50% of GAPDH expression (Fig. 1B, Right); however, virus-induced cell death was not detected (SI Appendix, Fig. S1). As shown in Fig. 1C, all cells produced detectable levels of vRNA after 24 h, with NPCs producing more viral genomes than pMGLs, consistent with the envelope staining.

DENV, a flavivirus closely related to ZIKV, is transmitted by the same mosquito vectors but is not known to be overtly teratogenic, although there are indications that it can be neurotropic and neurovirulent (19). To define the different pathogenicity of these related viruses we exposed the same cell types to DENV2. Fig. 1D shows that, while the virus infected and replicated in all cell types, the maximum DENV2 vRNA levels at 24 h were generally lower than those of ZIKV in the same cells, except in pMGLs where they reached 17% of GAPDH. To assess the kinetics of virus replication, we compared ZIKV[u] and DENV2 vRNA levels at different times after infection. As shown in Fig. 1E, ZIKV[u] vRNA levels changed rapidly from 24 to 72 h after infection, increasing 30-fold in NPCs (Left), 13-fold in astrocytes (Middle), and 9-fold more in pMGLs (Right). In contrast, DENV2 vRNA levels were lower at 24 h and appeared to decrease over the next 2 d (Fig. 1F). These results suggest that these cell types limit infection and replication of DENV2, while ZIKV[u] replication is exponential during this time.

The results in Fig. 1 E and F suggest that antiviral responses to infection are different for each virus, limiting DENV2 but
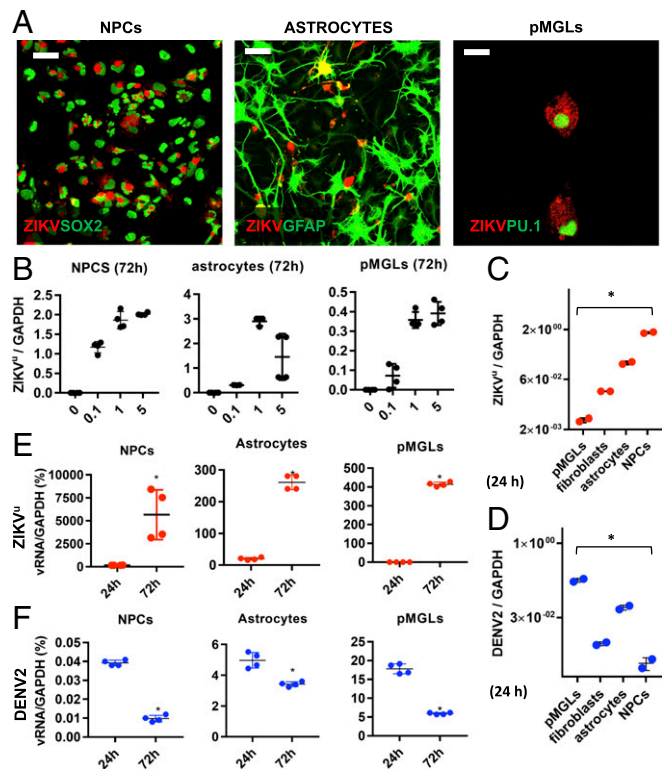
Fig. 1. ZIKV and DENV display different tropism and kinetics. (A, Left) Sox2+ (green, nuclear) iPS-derived NPCs infected with ZIKV (red, envelope staining). (Scale bar, 40 μm.) (Middle) GFAP+ (green, cytoplasmic) iPS-derived astrocytes derived from the same parental line display cytoplasmic ZIKV inclusions (red, envelope staining). (Scale bar, 40 μm.) (Right) PU.1+ microglia (green, nuclear) derived from the same parental line, also got infected with ZIKV and display numerous cytoplasmic foci positive for ZIKV envelope (red channel). (Scale bar, 12 μm.) (B) Dose-dependent infection of different cell types with ZIKV[u]. qPCR of ZIKV RNA (normalized to GAPDH) as a function of input inoculum MOI (Left, NPCs; Middle, astrocytes; Right, pMGLs). $n = 4$ technical replicates. (C) qPCR of ZIKV RNA at 24 h after infection of indicated cell types with inoculum (MOI 1), normalized to GAPDH. $n = 2$ technical replicates. (D) qPCR of DENV RNA at 24 h after infection of indicated cell types with viral inoculum (MOI 1), normalized to GAPDH. $n = 2$ technical replicates. *$P < 0.0001$ for ANOVA with post hoc Tukey test. (E) Kinetics of viral RNA accumulation (as percentage of GAPDH) between 24 and 72 h post-infection (hpi) with ZIKV inoculum (MOI 1) in isogenic NPCs (Left), astrocytes (Middle), and pMGLs (Right). *$P < 0.05$ for unpaired two-tailed t test. (F) Kinetics of viral restriction between 24 h and 72 h postinfection with DENV inoculum (MOI 1) in isogenic NPCs (Left), astrocytes (Middle), and pMGLs (Right). *$P < 0.05$ for unpaired two-tailed t test. (B–F) Error bars are mean ± SD (technical replicates).

allowing ZIKV[u] amplification. We assessed the effect of IFN pathways stimulation and inhibition on viral accumulation. When B18R, an inhibitor of type I IFN sensing and signaling, was added to infected cultures, ZIKV[u] replication was significantly increased after infection of astrocytes and microglia, and more marginally in NPCs (Fig. 2A). Conversely, when infected cultures were exposed to recombinant IFN-γ as an agonist of the type II IFN pathway, virus production was inhibited in all three cell types (Fig. 2A). In striking contrast, DENV2 did not increase in response to B18R, and was not inhibited by IFN-γ in any of the cell types (Fig. 2B). As shown in SI Appendix, Fig. S2, IFN-γ treatment of ZIKV[u]-infected NPCs efficiently protected these cells from infection and cell death.

To investigate whether the two viruses elicit different antiviral responses in infected cells, we measured gene expression of canonical viral sensors and downstream IFN-stimulated genes (ISGs). RIG-I is a dsRNA helicase acting as a primary sensor of
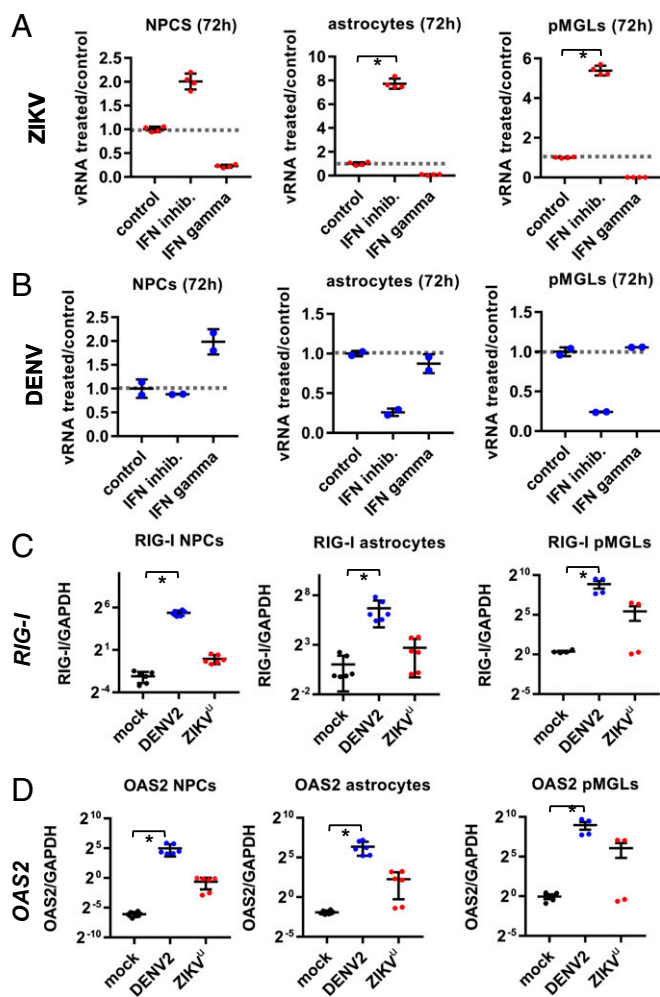
Fig. 2. Different IFN responses to ZIKV and DENV infection. (*A*) At 72 h postinfection, type I IFN inhibition by B18R increased ZIKV load (*Middle*) compared with control infection, while type II IFN activation by IFN-γ (*Right*) decreased ZIKV load (normalized to control ZIKV infection, *Left* and dashed line at 1), in isogenic NPCs (*Left*), astrocytes (*Middle*), and pMGLs (*Right*). $n = 4$ technical replicates. *$P < 0.05$ for ANOVA with post hoc Tukey test. (*B*) Effect of type I IFN inhibition (B18R, *Middle*) and type II IFN activation (IFN-γ, *Right*) on DENV viral load (normalized to control DENV infection, *Left* and dashed line at 1) in isogenic NPCs (*Left*), astrocytes (*Middle*), and pMGLs (*Right*). $n = 2$ technical replicates. (*C* and *D*) qPCR for the viral sensor *RIG-I* (*C*) and effector *OAS2* (*D*) following infection with DENV and ZIKV in isogenic NPCs (*Left*, $n = 6$), astrocytes (*Middle*, $n = 6$), and pMGLs (*Right*, $n = 4$). *RIG-I* and *OAS2* are significantly induced by DENV in all cells, and by ZIKV only in pMGLs. Gene expression is quantified 24 h postinfection and expressed normalized to *GAPDH*. Error bars are mean ± SD. *$P < 0.05$ for ANOVA with post hoc Tukey test.

invasion by multiple viruses (20), including DENV and other flaviviruses. OAS2 is an IFN-inducible enzyme which, in the presence of dsRNA, synthesizes an activator of RNase L acting as an effector of viral genome degradation and replication inhibition (21). Fig. 2*C* shows that *RIG-I* was induced within 24 h of exposure to DENV2 (blue data points in each graph) relative to control (black data points) in NPCs (*Left*), astrocytes (*Middle*), and microglia (*Right*), but *RIG-I* levels remained very low in both astrocytes and NPCs when exposed to ZIKV[u] (red data points) at a MOI that resulted in robust viral infection and replication and caused death of NPCs. Interestingly, ZIKV[u] triggered *RIG-I* up-regulation in pMGLs, likely owing to the specialized role of these cells as innate immune effectors. Similarly, *OAS2* was

induced in all three cell types by exposure to DENV2 (Fig. 2*D*) and in pMGLs only by ZIKV[u].
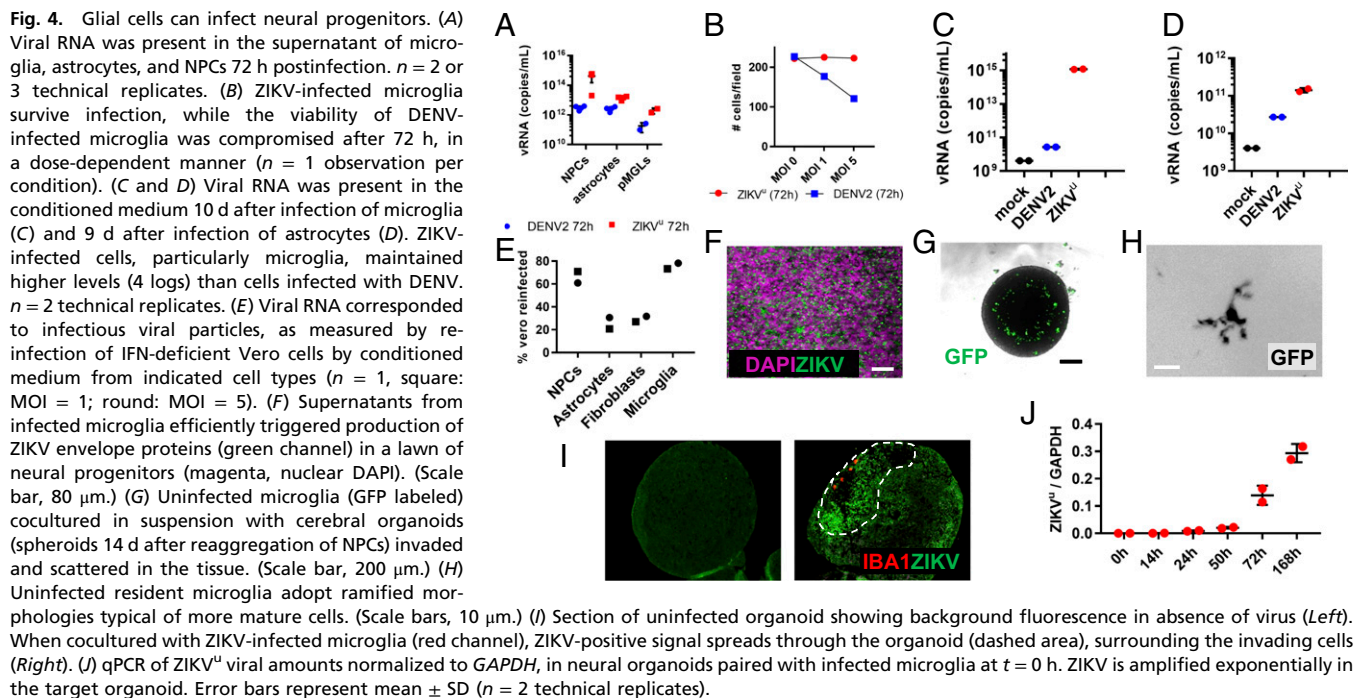
To assess more broadly the baseline antiviral capabilities of the different cell types, we measured expression of *RIG-I*, *MDA5*, *OAS2*, and *MX1* in absence of infection. As shown in Fig. 3*A*, NPCs had the lowest average levels of expression of these antiviral response genes, while pMGLs displayed the highest average. Fig. 3*B* shows that, in contrast to pMGLs exposed to ZIKV[u], pMGLs exposed to DENV2 (middle blot) expressed and secreted cytokines and chemokines whose combined action could be further involved in neuroinflammatory processes (such as CXCL10, see blot map in Fig. 3*C*) and elicit cytotoxic effects to defend the host. We observed that these early differences in cytokine release are not accompanied by a delayed rise in CXCL10 or IL6 transcription after ZIKA infection, but rather an apparent resolution (*SI Appendix*, Fig. S3) in both cases.

To understand virus pathogenesis, it is crucial to define the cell type that initiates and propagates virus in the fetus after primary infection of the mother. As a surrogate for virus production, we tested the supernatant of infected pMGLs, astrocytes, and NPCs for the presence of vRNA. As shown in Fig. 4*A*, the supernatants of pMGLs, astrocytes, and NPCs infected with either DENV2 or ZIKV[u] contained vRNA after 72 h, consistent with virus shedding and with ZIKV[u]-infected NPCs producing high levels before death. Remarkably, we observed that DENV2 was cytotoxic to pMGLs, in contrast to ZIKV[u], which did not induce cell number loss within 3 d of infection (Fig. 4*B*) but rather allowed release of viral genomes more than a week after initial infection (Fig. 4*C*). Large concentrations of ZIKV[u] vRNA could be detected more than a week after initial infection of astrocytes, while DENV2 genome release was significantly lower (Fig. 4*D*).

To test for the presence of active virus, beyond the vRNA presence, we exposed IFN-deficient Vero cells to the supernatant of the infected human cells. Fig. 4*E* shows that the supernatant from ZIKV[u]-infected microglia was efficient in establishing infection of Vero cells, as was the supernatant from infected NPCs. When neural progenitors, thought to represent the most relevant target cells for teratogenesis, were exposed to the supernatants of infected microglia, they became homogenously positive for ZIKV envelope protein (Fig. 4*F*) consistent with the possibility that primitive macrophages and microglia could initiate infection of the fetal brain.
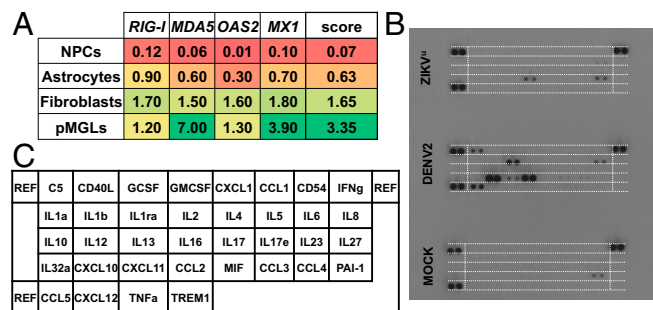
Fig. 3. (*A*) Expression levels (qPCR) of a panel of four main effectors of IFN signaling (*RIG-I*, *MDA5*, *OAS2*, and *MX1*) and their averages in four relevant cell types (NPCs, astrocytes, pMGLs, and human skin fibroblasts). Color ranges from red (0% *GAPDH*) to green (7% *GAPDH*). We measured the average of these four genes, as an IFN-defense score. NPCS have very low basal mean expression of all four genes (average 0.07), while pMGLs have high basal mean expression (average 3.35). (*B*) Cytokine profiles of microglia infected with ZIKV and DENV (medium conditioned from 12 hpi to 24 hpi). DENV induced the release of cytokines/chemokines typical of macrophage activation (CCL5, C5, and CXCL10). In contrast, ZIKV elicited the release of fewer cytokines/chemokines (CCL2 and IL8). (*C*) Map of cytokines and chemokines array probed in *B*, equivalent to the dashed white lines.

NEUROSCIENCE

Fig. 4. Glial cells can infect neural progenitors. (*A*) Viral RNA was present in the supernatant of microglia, astrocytes, and NPCs 72 h postinfection. n = 2 or 3 technical replicates. (*B*) ZIKV-infected microglia survive infection, while the viability of DENV-infected microglia was compromised after 72 h, in a dose-dependent manner (n = 1 observation per condition). (*C* and *D*) Viral RNA was present in the conditioned medium 10 d after infection of microglia (*C*) and 9 d after infection of astrocytes (*D*). ZIKV-infected cells, particularly microglia, maintained higher levels (4 logs) than cells infected with DENV. n = 2 technical replicates. (*E*) Viral RNA corresponded to infectious viral particles, as measured by re-infection of IFN-deficient Vero cells by conditioned medium from indicated cell types (n = 1, square: MOI = 1; round: MOI = 5). (*F*) Supernatants from infected microglia efficiently triggered production of ZIKV envelope proteins (green channel) in a lawn of neural progenitors (magenta, nuclear DAPI). (Scale bar, 80 μm.) (*G*) Uninfected microglia (GFP labeled) cocultured in suspension with cerebral organoids (spheroids 14 d after reaggregation of NPCs) invaded and scattered in the tissue. (Scale bar, 200 μm.) (*H*) Uninfected resident microglia adopt ramified morphologies typical of more mature cells. (Scale bars, 10 μm.) (*I*) Section of uninfected organoid showing background fluorescence in absence of virus (*Left*). When cocultured with ZIKV-infected microglia (red channel), ZIKV-positive signal spreads through the organoid (dashed area), surrounding the invading cells (*Right*). (*J*) qPCR of ZIKV^u viral amounts normalized to *GAPDH*, in neural organoids paired with infected microglia at t = 0 h. ZIKV is amplified exponentially in the target organoid. Error bars represent mean ± SD (n = 2 technical replicates).

To model the ability of infected microglial precursors (primitive macrophages) to migrate into the developing CNS and spread ZIKV to vulnerable cells, we developed a 3D-culture model expanding on our initial work replicating an organotypic environment for microglia (18, 22, 23). Fig. 4*G* shows that immature GFP-labeled pMGLs, paired with a neuralized organoid, actively migrate into the growing tissue, taking residence and eventually adopting the ramified morphology of more mature microglial cells (Fig. 4*H*). When pMGLs that were preinfected with ZIKV^u were cocultured with uninfected organoids (Fig. 4*I*, *Right*), we found that invading pMGLs penetrated the tissue and could be detected below the surface of the neural tissue as large amoeboid cells filled with granular phagocytic content, positive for Iba1, and reminiscent of the Gitter cell endpoint of microglia (24). Surrounding the invading pMGLs (red channel), we observed a zone of loose cellular structure displaying elevated ZIKV envelope signal interspersed with pyknotic and fragmented nuclei, indicative of an ongoing degenerative process (green, dashed loop). For reference, we verified that direct infection with a ZIKV inoculum of a similar-sized organoid, resulted in stalled growth (*SI Appendix*, Fig. S4*A*), as previously reported (25, 26). Fig. 4*J* depicts the increase in viral load in the target organoid, in the days following pairing with infected pMGLs. Higher magnification of organoid sections showed that the ZIKV-positive microglial cells initiated infection of adjacent cells, as exemplified by the large ZIKV-positive cytoplasmic inclusions found in nearby parenchymal cells (*SI Appendix*, Fig. S4*B*, *Right*, yellow arrowheads, all panels).

Astrocytes are, in intimate partnership with endothelial cells, the primary components of the blood–brain barrier (BBB) defining the specialized immune environment of the CNS (27), preventing entry of pathogens and immune cells. We compared viral cytotoxicity to astrocytes and endothelial cells, exposing homogenous cultures to ZIKV^u and DENV2. As shown in Fig. 5*A*, *Middle* DENV2 exposure was cytotoxic to astrocytes, decreasing density, and rapidly (<24 h) triggered apoptotic cell death (*SI Appendix*, Fig. S5). In contrast, ZIKV^u only caused an increase in GFAP staining (Fig. 5*A*, *Right*), characteristic of astrogliosis (28) without changes in cell density (*SI Appendix*, Fig.

S5). Endothelial cells infected with DENV2 or ZIKV^u (Fig. 5*B*) displayed faint and fragmented ZO-1 staining, indicating a disruption of tight junctions' continuity, which is essential to the endothelial barrier role. This disruption may be relevant to the consequences of postnatal infections, including infections in the adult human. Indeed, as shown in Fig. 5*C*, neuronal cultures could be efficiently infected with ZIKV in a dose-dependent manner. To assess whether virus infection could cause functional impairment, we infected cultures grown on multielectrode arrays. As shown in Fig. 5 *D* and *E*, infections with DENV2 or ZIKV^u induced a rapid loss of electrophysiological activity. Strikingly, DENV2-infected neurons recovered, and resumed activity spontaneously (Fig. 5*E*), indicating that DENV2 can be neurotoxic, but functional impairment is reversible at the cellular level. In the tested conditions of infection, ZIKV-infected neurons did not recover, eventually degenerating (*SI Appendix*, Fig. S6).

Discussion

As is the case with DENV infection, ZIKV has been known to result in a self-limiting and mild disease in most adult patients, with rashes and fevers being the most common symptoms (29). While DENV sometimes leads to a grave hemorrhagic syndrome (16, 30), and in rare cases to neurological damage, maternal ZIKV infection during early stages of pregnancy can often result in fetal neurological abnormalities, ranging from inflammatory scarring with calcifications to severe microcephaly at birth (3, 31). It is currently unknown how ZIKV crosses all maternal–fetal defenses and barriers to reach the fetal CNS, why virus infection during the first trimester is most damaging (5), or why the closely related flavivirus DENV does not cause fetal brain injury. Although great success has already come from the study of ZIKV in pluripotent stem cell-derived cultures (6–9, 32), both viruses are difficult to model in mice, unless IFN defenses are ubiquitously ablated (33, 34). Here we show that ZIKV^u is under tighter IFN restriction than DENV2 in all studied cells (Fig. 2), and that cells which are highly vulnerable, such as neural progenitors, have low baseline defenses (Fig. 3) and are unable to mount an efficient response before viremia slows growth or
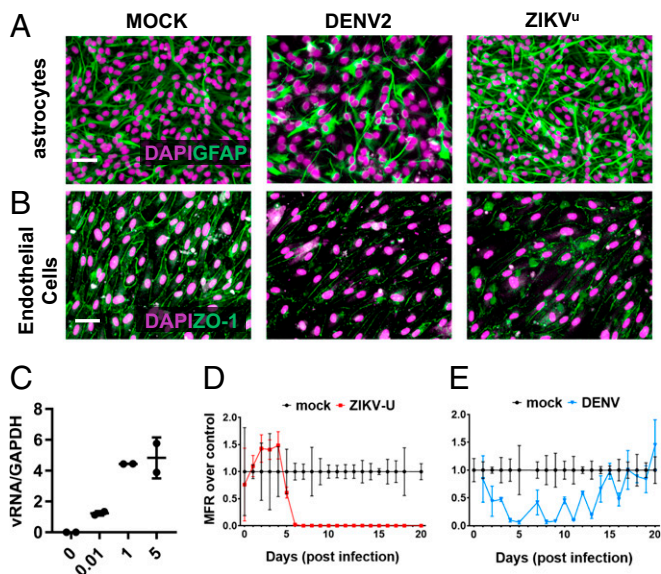
Fig. 5. Modeling the postnatal effects of CNS infection. (*A*) Astrocytes responded differently to DENV and ZIKV challenges. DENV promoted a loss of viability (*Middle*, DAPI staining), and an overall decrease of GFAP staining (*Middle*, green channel). In contrast, ZIKV did not alter cell numbers (*Right*), but triggered a relative increase in GFAP staining intensity, characteristic of astrogliosis. (Scale bar, 40 μm.) (*B*) Blood–brain barrier modeled with a confluent culture of iPS-derived endothelial cells, forming a network of ZO-1 positive tight junctions (green channel, *Left*). Both DENV (*Middle*) and ZIKV (*Right*) elicited a loss of ZO-1 staining intensity. (Scale bar, 40 μm.) (*C*) A mixed culture of neurons differentiated for 4 wk could be efficiently infected by ZIKV, in an input MOI-dependent manner (ZIKV RNA normalized to *GAPDH*) (*n* = 2 technical replicates). (*D*) Neuronal culture, infected with ZIKV at electrophysiological maturity (6 wk, day 0 of *x* axis), displayed a rapid and irreversible drop in action potential firing rate (red trace) compared with control (black trace). (*E*) In contrast, DENV infection resulted in a reversible loss of spontaneous electrical activity (blue trace), reverting to control levels of activity (black trace) after 2 wk. (*D* and *E*) Values are mean ± SEM (*n* = 5 technical replicates for controls, 3 for ZIKV^u, 2 for DENV).

triggers death. We also show that microglia-like cells can be productively infected and show little cytotoxicity (Figs. 1–3 and *SI Appendix*, Fig. S1), even when infected with high titers of ZIKV. In contrast, DENV triggers cytotoxic reactions in microglia-like cells, as has been reported for other myeloid cells (35).

Our results suggest that DENV can be efficiently restricted by the IFN responses it triggers: this suggests it may more rarely reach distant tissue (host brain, fetal brain). In the fetus, primitive macrophages/immature microglia, would make poor vectors for DENV, as these cells are highly vulnerable to DENV infection. In contrast, ZIKV may have evolved an optimal set of characteristics, allowing it to replicate and propagate in myeloid cells, culminating in infection of microglial precursors without causing serious cytotoxic effects, giving them time to propagate the virus to the tissues they encounter. At the maternal–fetal boundary, cytotrophoblast cells and Hofbauer cells, residing in the chorionic villi, can be infected by ZIKV (36, 37). ZIKV can reach these cells through the chorioallantoic placenta or the highly vascularized yolk sac splanchnopleure. Our work suggests that microglial precursors migrating between the blood islands of the yolk sac (where they originate) and the embryo proper may represent attractive candidate cells that are susceptible to infection, able to transport the virus to the CNS, and mediate infection of neural progenitors (Fig. 6).

Timing of infection into microglial precursors migrating to the CNS, before closure of the BBB, may be among the mechanisms

enhancing teratogenicity in the first trimester. In vivo evidence of such an event is not currently available, although microglia have been shown to be susceptible to infection in several models, including fetal human slice cultures (38), human fetal brain preparations (39), and nonhuman primates (40). The general reliance of mouse models on blunted IFN defenses to observe any pathogenicity of ZIKV hinders direct assessment of this transfer hypothesis. However, striking circumstantial support can be found in a recent study (41) using immunocompetent mice, bypassing most of the host defenses using intrauterine injections of the virus. In this study, the authors showed that ZIKV, injected at embryonic day 10 (E10), could later be found in the fetal mouse brain, more specifically in microglia where it triggered their activation. Remarkably, when injection was performed later, at E14, the virus failed to reach the fetal CNS. It should be noted that at E10, yolk sac microglial precursors are entering the CNS, while at E14, this emigration is complete (42). We note that pMGLs, in contrast to NPCs, can still mount a response to the virus: in certain circumstances they may help limit viral spread in the CNS parenchyma, for example, at later stages when more mature and present at higher density. A study published while this manuscript was under review (43), supporting many of our own findings, suggest this may indeed be the case: cocultures of NPCs and iPS-derived macrophages demonstrated less viral positivity than NPCs alone after exposure to ZIKV. The authors concluded there was active removal of infected NPCs by macrophages, highlighting the complex interplay between their role as vectors and as protective actors.

AXL is an attractive candidate receptor for the virus (44, 45), although AXL ablation was recently found to have no effect on
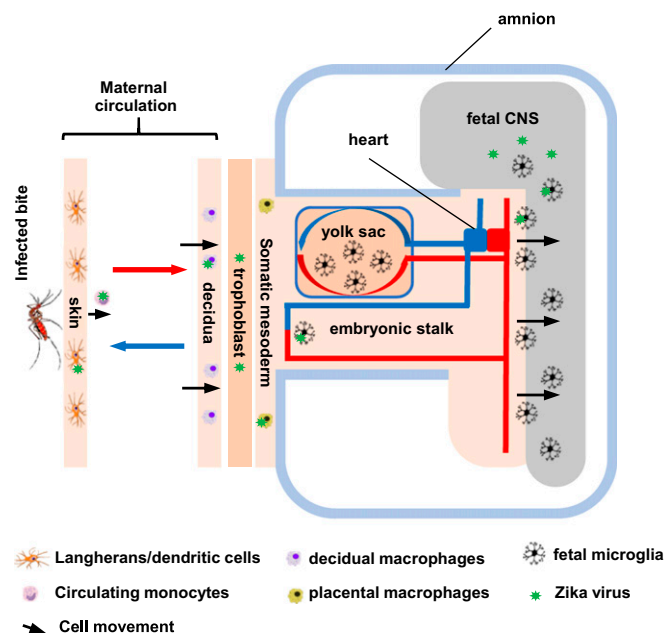
Fig. 6. Diagram of the proposed maternal–fetal myeloid chain of ZIKV transmission, from skin macrophages (Langerhans and dendritic cells) all the way to the fetus. Virus from pools of infected decidual maternal macrophages break through placental defenses. Placental fetal resident macrophages get infected but do not travel or come in physical contact with the fetal CNS. Microglial precursors, migrating past the placental and vitelline exchange endothelia, get infected on their way to the embryo, invading the neural tube at its most vulnerable stage. Migration eventually stops, and the blood–brain barrier closes. ZIKV-infected immune cells may constitute a viral reservoir for sustained periods. In contrast, DENV may never reach the fetal neighborhoods, actively restricted in the maternal host, or triggering cell death in microglia precursors it reaches.

the behavior of ZIKV toward neural progenitors (46), and AXL is dispensable for infection in the mouse (34). Other entry mechanisms active in myeloid cells such as microglia include Fc receptors that may allow enhanced endocytosis of virions in the presence of antibodies with partial avidity for ZIKV (1, 47–49). An interesting implication would be that cross-reactive maternal antibodies, some of which may come from previous DENV infections and are present in the fetus, will favor viral infection of primitive myeloid cells such as microglia, further enhancing delivery to the fetal brain (47–49). In the adult, prior DENV infections may leave the BBB vulnerable while also enhancing ZIKV infectivity. We show that DENV2 and ZIKV^u may alter the integrity of elements of the BBB, disturbing tight junctions between endothelial cells. Interestingly, it was recently observed that ZIKV protein NS2A can disrupt adherent junctions in radial glial cells (6). We also show ZIKV can activate astrocytes, while DENV2 is actively cytotoxic. Finally, we observed that ZIKV can permanently damage electrophysiologically active neuronal networks, consistent with viral toxicity in the adult (2), which may be aggravated in cases of coinfection. Ultimately, astrocytes and microglia may become long-term viral reservoirs in the absence of efficient clearing mechanisms, and the consequences of such events remain to be investigated. Our data suggest that type I and II IFN modulation may represent an attractive treatment target, as the teratogenicity of ZIKV may rely on latent vulnerabilities of target cell types (NPCs), evading IFN-dependent eradication in cells such as microglia and astrocytes that may act as Trojan horses or even as viral reservoirs.

Materials and Methods

For a complete description of the materials and methods used in this paper, please refer to *SI Appendix*. Virus stocks of DENV2 and ZIKV^u were produced in Vero and C6/36 cells. Microglia and neural progenitors were differentiated from iPS cells and neural progenitors were used to generate astrocytes, neurons, and neural organoids.

All experiments involving cells from human donors and animals were performed in compliance with established IRB protocols at the Whitehead institute.

1. Li H, Saucedo-Cuevas L, Shresta S, Gleeson JG (2016) The neurobiology of Zika virus. *Neuron* 92:949–958.
2. Cao-Lormeau VM, et al. (2016) Guillain-Barré syndrome outbreak associated with Zika virus infection in French Polynesia: A case-control study. *Lancet* 387:1531–1539.
3. Martines RB, et al. (2016) Pathology of congenital Zika syndrome in Brazil: A case series. *Lancet* 388:898–904.
4. Mlakar J, et al. (2016) Zika virus associated with microcephaly. *N Engl J Med* 374: 951–958.
5. Roberts DJ, Frosch MP (2016) Zika and histopathology in first trimester infections. *Lancet* 388:847–849.
6. Yoon KJ, et al. (2017) Zika-virus-encoded NS2A disrupts mammalian cortical neurogenesis by degrading adherens junction proteins. *Cell Stem Cell* 21:349–358.e6.
7. Xu M, et al. (2016) Identification of small-molecule inhibitors of Zika virus infection and induced neural cell death via a drug repurposing screen. *Nat Med* 22:1101–1107.
8. Tang H, et al. (2016) Zika virus infects human cortical neural progenitors and attenuates their growth. *Cell Stem Cell* 18:587–590.
9. Ming GL, Tang H, Song H (2016) Advances in Zika virus research: Stem cell models, challenges, and opportunities. *Cell Stem Cell* 19:690–702.
10. Wang L, et al. (2016) From mosquitos to humans: Genetic evolution of Zika virus. *Cell Host Microbe* 19:561–565.
11. Yuan L, et al. (2017) A single mutation in the prM protein of Zika virus contributes to fetal microcephaly. *Science* 358:933–936.
12. Rossi SL, Vasilakis N (2016) Modeling Zika virus infection in mice. *Cell Stem Cell* 19:4–6.
13. Mysorekar IU, Diamond MS (2016) Modeling Zika virus infection in pregnancy. *N Engl J Med* 375:481–484.
14. Lazear HM, et al. (2016) A mouse model of Zika virus pathogenesis. *Cell Host Microbe* 19:720–730.
15. Soares CN, et al. (2016) Fatal encephalitis associated with Zika virus infection in an adult. *J Clin Virol* 83:63–65.
16. Olagnier D, et al. (2016) Dengue virus immunopathogenesis: Lessons applicable to the emergence of Zika virus. *J Mol Biol* 428:3429–3448.
17. Soldner F, Jaenisch R (2012) Medicine. iPSC disease modeling. *Science* 338:1155–1156.
18. Muffat J, Li Y, Jaenisch R (2016) CNS disease models with human pluripotent stem cells in the CRISPR age. *Curr Opin Cell Biol* 43:96–103.
19. Screaton G, Mongkolsapaya J, Yacoub S, Roberts C (2015) New insights into the immunopathology and control of dengue virus infection. *Nat Rev Immunol* 15:745–759.
20. Kell AM, Gale M, Jr (2015) RIG-I in RNA virus recognition. *Virology* 479–480:110–121.
21. Lin RJ, et al. (2009) Distinct antiviral roles for human 2′,5′-oligoadenylate synthetase family members against dengue virus infection. *J Immunol* 183:8035–8043.
22. Muffat J, et al. (2016) Efficient derivation of microglia-like cells from human pluripotent stem cells. *Nat Med* 22:1358–1367.
23. Li Y, et al. (2016) Induction of expansion and folding in human cerebral organoids. *Cell Stem Cell* 20:385–396.e3.
24. Das GD (1976) Gitter cells and their relationship to macrophages in the developing cerebellum: An electron microscopic study. *Virchows Arch B Cell Pathol Incl Mol Pathol* 20:299–305.
25. Garcez PP, et al. (2016) Zika virus impairs growth in human neurospheres and brain organoids. *Science* 352:816–818.
26. Qian X, et al. (2016) Brain-region-specific organoids using mini-bioreactors for modeling ZIKV exposure. *Cell* 165:1238–1254.
27. Obermeier B, Verma A, Ransohoff RM (2016) The blood-brain barrier. *Handb Clin Neurol* 133:39–59.
28. Yang Z, Wang KK (2015) Glial fibrillary acidic protein: From intermediate filament assembly and gliosis to neurobiomarker. *Trends Neurosci* 38:364–374.
29. Petersen LR, Jamieson DJ, Powers AM, Honein MA (2016) Zika virus. *N Engl J Med* 374: 1552–1563.
30. Halstead SB, Cohen SN (2015) Dengue hemorrhagic fever at 60 years: Early evolution of concepts of causation and treatment. *Microbiol Mol Biol Rev* 79:281–291.
31. Coyne CB, Lazear HM (2016) Zika virus–Reigniting the TORCH. *Nat Rev Microbiol* 14: 707–715.
32. Cugola FR, et al. (2016) The Brazilian Zika virus strain causes birth defects in experimental models. *Nature* 534:267–271.
33. Sarathy VV, Milligan GN, Bourne N, Barrett AD (2015) Mouse models of dengue virus infection for vaccine testing. *Vaccine* 33:7051–7060.
34. Miner JJ, et al. (2016) Zika virus infection in mice causes panuveitis with shedding of virus in tears. *Cell Rep* 16:3208–3218.
35. Martins Sde T, Silveira GF, Alves LR, Duarte dos Santos CN, Bordignon J (2012) Dendritic cell apoptosis and the pathogenesis of dengue. *Viruses* 4:2736–2753.
36. Tabata T, et al. (2016) Zika virus targets different primary human placental cells, suggesting two routes for vertical transmission. *Cell Host Microbe* 20:155–166.
37. Quicke KM, et al. (2016) Zika virus infects human placental macrophages. *Cell Host Microbe* 20:83–90.
38. Retallack H, et al. (2016) Zika virus cell tropism in the developing human brain and inhibition by azithromycin. *Proc Natl Acad Sci USA* 113:14408–14413.
39. Lum FM, et al. (2017) Zika virus infects human fetal brain microglia and induces inflammation. *Clin Infect Dis* 64:914–920.
40. Adams Waldorf KM, et al. (2016) Fetal brain lesions after subcutaneous inoculation of Zika virus in a pregnant nonhuman primate. *Nat Med* 22:1256–1259.
41. Vermillion MS, et al. (2017) Intrauterine Zika virus infection of pregnant immunocompetent mice models transplacental transmission and adverse perinatal outcomes. *Nat Commun* 8:14575.
42. Ginhoux F, Guilliams M (2016) Tissue-resident macrophage ontogeny and homeostasis. *Immunity* 44:439–449.
43. Mesci P, et al. (2017) Modeling neuro-immune interactions during Zika virus infection. *Hum Mol Genet* 27:41–52.
44. Hamel R, et al. (2015) Biology of Zika virus infection in human skin cells. *J Virol* 89: 8880–8896.
45. Nowakowski TJ, et al. (2016) Expression analysis highlights AXL as a candidate zika virus entry receptor in neural stem cells. *Cell Stem Cell* 18:591–596.
46. Wells MF, et al. (2016) Genetic ablation of AXL does not protect human neural progenitor cells and cerebral organoids from Zika virus infection. *Cell Stem Cell* 19: 703–708.
47. Dejnirattisai W, et al. (2016) Dengue virus sero-cross-reactivity drives antibody-dependent enhancement of infection with zika virus. *Nat Immunol* 17:1102–1108.
48. Durbin AP (2016) Dengue antibody and Zika: Friend or foe? *Trends Immunol* 37: 635–636.
49. Paul LM, et al. (2016) Dengue virus antibodies enhance Zika virus infection. *Clin Transl Immunology* 5:e117.